



# Volume production of high loading Pt/C catalyst with high performance via a microwave-assisted organic colloid route

Bin Liu<sup>a,b</sup>, Liping Zheng<sup>a,b</sup>, Shijun Liao<sup>a,b,\*</sup>, Jianhuang Zeng<sup>a,b</sup>

<sup>a</sup> School of Chemistry and Chemical Engineering, South China University of Technology, Guangzhou 510641, China

<sup>b</sup> Guangdong Provincial Key Lab for Fuel Cell Technology & Key Lab of Enhanced Heat Transfer and Energy Conservation, Ministry of Education, China

## ARTICLE INFO

### Article history:

Received 23 February 2012

Accepted 28 February 2012

Available online 7 March 2012

### Keywords:

Catalyst

Microwave-assisted organic colloid

Fuel cell

Volume production

## ABSTRACT

A scale-up preparation of high-loading Pt/C (40 wt%) to 3 g per pot has been achieved with a microwave-assisted organic colloid method, followed by appropriate heat treatment in alternating atmospheres (nitrogen, oxygen, and hydrogen). The catalysts prepared in this work were characterized by thermogravimetric analysis, X-ray diffraction analysis, and transmission electron microscopy etc., and were found to be competitive with state-of-the-art HiSPEC 4100 Pt/C catalyst in terms of their activities towards the anodic oxidation of methanol and the cathodic reduction of oxygen. They also displayed better cathodic activity and stability in a hydrogen/air single-cell test. The particle size was as small as 2.3 nm, which is smaller than HiSPEC 4100 Pt/C catalyst. The scale-up work reported in this paper provides a practicable method to achieve the volume production of a high-loading Pt/C catalyst for fuel cell applications.

© 2012 Elsevier B.V. All rights reserved.

## 1. Introduction

Electrocatalysts are one of the key materials currently hindering the development of low-temperature fuel cells [1–3]. These electrocatalysts contribute more than 30% to the total cost of a polymer electrolyte membrane fuel cell, due to their high platinum content. Much current research attention is therefore focused on the development of nano-sized platinum particles to achieve high platinum utilization. It is not difficult to prepare small amounts (i.e., milligrams) of high-loading Pt/C catalysts with particle sizes smaller than 3 nm, but it remains a challenge to realize volume preparation (in terms of grams per pot) of these same catalysts. Presently, the size of a state-of-the-art Pt/C catalyst produced by Johnson Matthey (40 wt.%, HiSPEC 4100) is around 3 nm. Thus, considerable effort has been expended to achieve the volume preparation of a high-loading Pt/C catalyst with a high surface area, high catalytic activity, and high platinum utilization [4,5].

Membrane electrode assemblies (MEAs) with thin catalyst layers have been developed in recent years because they can achieve high performance using small amounts of platinum. It is therefore desirable to prepare a catalyst with high platinum loading. In practice, commercially available fuel cells used catalyst loadings as high as 70%; however, in such cases the platinum particle size is up to 20 nm due to the high-loading catalyst's propensity toward self-agglomeration. Hence, it remains important to seek an appropriate

method for preparing a high Pt loading catalyst that can be used in practical applications [6].

To prepare a high Pt loading catalyst that is small and highly active, the majority of research studies have focused on optimizing catalyst synthesis procedures, since the particle size, uniformity, and dispersibility of the active components in electrocatalysts are strongly dependent on the preparation methods, such as the chemical impregnation-reduction method [7,8], the micro-emulsion method [9,10], and the colloidal method [11]. Although these traditional procedures have been applied to synthesize carbon-supported Pt catalysts with low metal loadings (usually less than 20 wt.%), they are ineffective for preparing high Pt loading catalysts because they result in large particles and uneven particle distribution.

Heat treatment after catalyst preparation has been recognized as an important and sometimes necessary step to improve catalytic activity [12–16], because it can remove some undesirable impurities from the early preparation stages, thereby achieving a uniform and stable dispersion of the metal on the support, and consequently enhancing the synthesized catalyst's activity. Heat treatment is usually conducted in an oven or furnace under one [17] or two [18,19] kinds of atmosphere. Gaseous atmospheres usually consist of high-purity N<sub>2</sub>, O<sub>2</sub>, or H<sub>2</sub>, or two of these combined.

In this paper, a microwave-assisted organic colloid approach was adopted to scale-up the synthesis of a Pt/C catalyst with high loading (40 wt.%). In the process, ethylene glycol (EG) was used as a solvent-cum-reducing agent and sodium citrate as a complexing agent. Subsequent heat treatment further enhanced the activity of the as-prepared catalyst. The catalyst prepared in this work was found to be competitive with state-of-the-art HiSPEC Pt/C in terms

\* Corresponding author at: School of Chemistry and Chemical Engineering, South China University of Technology, Guangzhou 510641, China. Tel.: +86 020 87113586. E-mail address: [chsjliao@scut.edu.cn](mailto:chsjliao@scut.edu.cn) (S. Liao).

of dispersion, particle size, methanol oxidation activity, and oxygen reduction activity.

## 2. Experimental

### 2.1. Catalyst preparation

#### 2.1.1. Carbon black pretreatment

Vulcan XC72 carbon black (Cabot Corp., BET:  $237\text{ m}^2\text{ g}^{-1}$ , denoted as C) was pretreated using a previously described procedure [20]. Briefly, the carbon black was first pretreated at room temperature in acetone. Then the carbon powder was subjected to refluxing in a mixture of hydrogen peroxide and nitric acid at  $80\text{ }^\circ\text{C}$  for 5 h to induce hydrophilic moieties and remove any possible metal residues. Finally, the carbon black was filtered, then vacuum dried at  $80\text{ }^\circ\text{C}$  overnight before use.

#### 2.1.2. Catalyst preparation

The process used to prepare the Pt/C catalyst was as follows. First, sodium citrate was dissolved in 50 mL ethylene glycol under stirring for 3 h. Afterwards, ethylene glycol solution containing a calculated amount of hexachloroplatinic acid ( $\text{H}_2\text{PtCl}_6 \cdot 6\text{H}_2\text{O}$ ) was added. Next, 2.5 g pre-treated carbon powder was then added to the mixture, followed by pH adjustment to 9 by the drop-wise addition of 5 wt.% KOH/EG solution under vigorous stirring. The mixture was then transferred in a conical flask into the center of a microwave oven (2450 MHz, 800 W) equipped with a condenser and was subjected to microwave heating for 220 s. After the mixture returned to room temperature, 10 wt.%  $\text{HNO}_3$  was added to adjust the solution pH to 3, followed by filtering, washing, and vacuum drying at  $90\text{ }^\circ\text{C}$ . The post-treatment was conducted as follows: the powdered solid, shielded in a  $\text{N}_2$  atmosphere, was first heated for 4 h at  $100\text{ }^\circ\text{C}$ , then for 30 min at  $100\text{ }^\circ\text{C}$  under a mixed  $\text{N}_2/\text{O}_2$  atmosphere (volume ratio, 90:10). Finally, the catalyst was treated for 1 h at  $100\text{ }^\circ\text{C}$  under a mixed  $\text{N}_2/\text{H}_2$  atmosphere (volume ratio: 90/10). The as-prepared catalyst was denoted as MW-PC and the heat-treated catalyst as H-MW-PC, where MW indicates microwave-assisted and PC indicates platinum on the carbon support. A Johnson Matthey HiSPEC 4100 Pt/C catalyst (40 wt.%), denoted as JM-PC, was used for comparison.

### 2.2. Catalyst characterization

UV–visible (UV–vis) spectra in the region of 220–800 nm were recorded by a Shimadzu UV-2501 spectrophotometer during the course of platinum precursor reduction. X-ray powder diffraction (XRD) was carried out on a Shimadzu XD-3A, using filtered Cu K $\alpha$  radiation and operating at 35 kV and 30 mA. The  $2\theta$  region between  $20^\circ$  and  $80^\circ$  was explored at a scan rate of  $4^\circ\text{ min}^{-1}$ . Thermogravimetric analysis (TGA) was performed using a Q500 TGA analyzer (TA Instruments, UK) to examine the metal loading. The morphology of the catalyst was observed using a transmission electron microscope (TEM; JEOL JEM-2010 HR) operated at 200 kV.

### 2.3. Electrochemical evaluation of the catalysts

Electrochemical measurements were carried out at room temperature using an electrochemical work station (Ivium, Netherlands). A common three-electrode electrochemical cell was used for the measurements. A platinum wire and an Ag/AgCl electrode were used as the counter and reference electrodes, respectively. The working electrode was a glassy carbon disk (5 mm in diameter) covered with a thin layer of Nafion-impregnated catalyst. The thin-film layer was prepared as follows: 5.0 mg of catalyst was dispersed ultrasonically in 1.0 mL Nafion/ethanol (0.25 wt.% Nafion) for 30 min. Then 5  $\mu\text{L}$  ink solution was pipetted and spread on the glassy carbon surface and the electrode was air dried. Cyclic

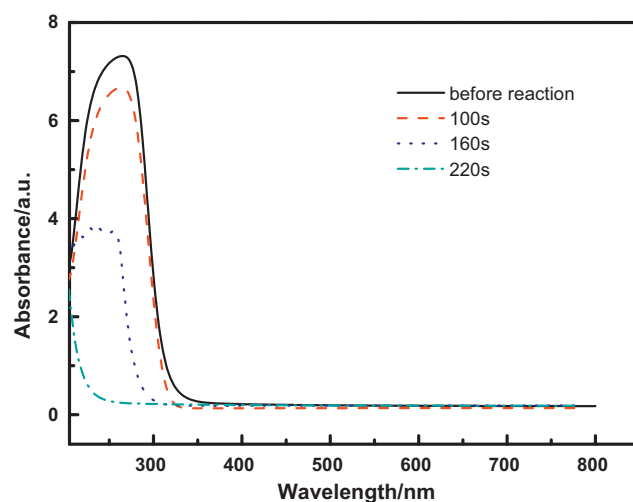


Fig. 1. UV–vis spectra of solutions before and during the reduction reaction of the Pt precursor.

voltammetry curves were obtained in  $0.5\text{ mol L}^{-1}\text{ H}_2\text{SO}_4$  for electrochemical active surface area measurements, and the catalytic activity evaluation was carried out in a solution of  $0.5\text{ mol L}^{-1}\text{ H}_2\text{SO}_4 + 0.5\text{ mol L}^{-1}\text{ CH}_3\text{OH}$  in the potential range of  $-0.2$  to  $1.0\text{ V}$  at a scan rate of  $50\text{ mV s}^{-1}$ . Linear sweep voltammetry (LSV) tests were conducted in  $0.5\text{ mol L}^{-1}\text{ O}_2$ -saturated  $\text{H}_2\text{SO}_4$  solution in the potential range of  $1$ – $0.2\text{ V}$  and at a scan rate of  $0.002\text{ V s}^{-1}$ . The electrode was rotated at 1600 rpm for this measurement.

### 2.4. MEA fabrication and single-cell test

To fabricate the MEA, an appropriate amount of catalyst powder was mixed with a solution of Nafion and isopropyl alcohol, then the mixture was dispersed ultrasonically to form a homogeneous ink. Afterwards, the catalyst ink was sprayed onto each side of a Nafion membrane (NR212), followed by hot pressing of the coated Nafion membrane with hydrophobically treated carbon paper. Three pieces of MEA were fabricated for comparison. All the MEAs used JM-PC as their anode catalyst. With respect to the cathode catalyst, one MEA was prepared with JM-PC, and the other two were prepared with either MW-PC or H-MW-PC as the cathode catalyst. Therefore, the performance of each MEA reflected the catalytic activity of its cathode catalyst. The anode and cathode catalyst loadings were  $0.1\text{ mg cm}^{-2}$  and  $0.2\text{ mg cm}^{-2}$ , respectively.

The  $\text{H}_2$ – $\text{O}_2$  single fuel cell was operated under the following conditions: high purity hydrogen and compressed air were fed into the single cell at 30 psi, and the cell operating temperature was set at  $70\text{ }^\circ\text{C}$ . The MEA was conditioned for 3 h in discharge mode at  $70\text{ }^\circ\text{C}$  before data acquisition.

## 3. Results and discussion

The formation of Pt colloids via this microwave-assisted organic colloid route was monitored by UV–vis spectroscopy. Fig. 1 shows the UV–vis spectra taken at different times (100, 160, and 220 s) during the preparation of the Pt colloids. The precursor solution, which was pale yellow before reduction, displays a peak at 260 nm as a result of ligand-to-metal charge-transition in the  $\text{PtCl}_6^{2-}$  ion [21,22]. As expected, this peak decreases with the proceeding reaction time during the course of the platinum precursor reduction. The peak is no longer visible after 220 s, suggesting that all the  $\text{PtCl}_6^{2-}$  ions had been completely reduced. Therefore, after 220 s of microwave irradiation, there should have been no Pt precursor left.

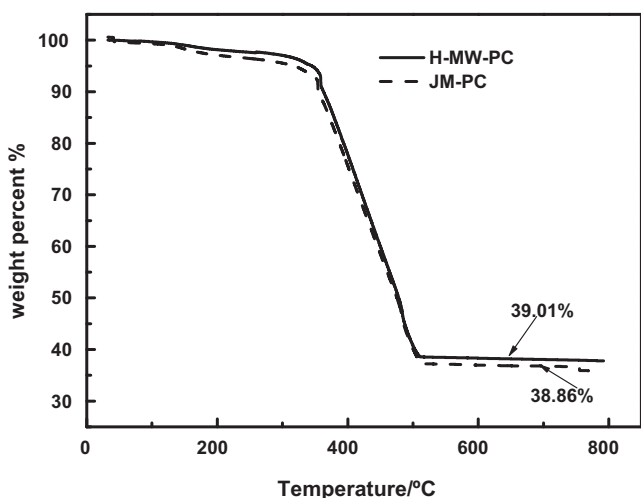


Fig. 2. TGA curves of H-MW-PC and JM-PC catalysts under air flow at a heating rate of  $10^{\circ}\text{C min}^{-1}$ .

TGA can be used to determine the Pt loading in Pt/C catalysts. To remove water that may have been physically adsorbed, the samples were vacuum dried at  $100^{\circ}\text{C}$  for 10 h before TGA. Fig. 2 shows the thermogravimetric curves in air flow for the H-MW-PC and JM-PC catalysts. The mass loss between  $380^{\circ}\text{C}$  and  $510^{\circ}\text{C}$  is due to calcination of the carbon support in air [23], and the curves tend to level above  $510^{\circ}\text{C}$  as a result of residual Pt. The Pt loading of the H-MW-PC catalyst is calculated to be 39.0 wt.%, in fair agreement with the nominal loading (40 wt.%). This result also signifies the complete reduction of the Pt precursor under the current experimental conditions, further confirming the UV–vis spectra findings discussed above. The commercial JM-PC catalyst was found to contain 38.9 wt.% Pt, quite consistent with the specified loading (39–41 wt.%).

Fig. 3A shows the XRD patterns of the H-MW-PC and JM-PC catalysts. The peak at  $2\theta = 25^{\circ}$  can be attributed to the Vulcan XC72 carbon support. The peaks located at  $2\theta = 39.7^{\circ}$ ,  $46.2^{\circ}$ , and  $67.4^{\circ}$  are ascribed to Pt (1 1 1), Pt (2 0 0), and Pt (2 2 0), which is characteristic of a face-centered cubic (fcc) structure. It has been reported that the electrocatalytic activity for the oxygen reduction reaction at the Pt (2 0 0) lattice plane is higher than for the other lattice planes, and that the Pt (2 0 0) crystal plane is the main active center for oxygen reduction [24]. More exposed Pt (2 0 0) lattice planes are indicative of more reactive atoms participating in the reduction of oxygen. The proportion of lattice planes can be calculated using the expression  $I_{hkl}/I_0$ . Fig. 3B shows the difference between the  $I_{hkl}/I_0$  values for the two samples. The H-MW-PC catalyst has a Pt (2 0 0) lattice plane proportion of 35%, higher than the commercial JM-PC catalyst (27%), predicting that the former will have better oxygen reduction catalytic activity. The Pt (2 0 0) diffraction peak was used to calculate the volume-averaged particle sizes of the Pt/C nanoparticles according to the Debye–Scherrer formula [25]; the average sizes for the two catalysts are comparable (about 2.5 nm).

Fig. 4 shows the TEM images together with the particle size distribution of the H-MW-PC catalyst. It can be seen that the active components are highly dispersed on the carbon supports and the particle size distribution is quite uniform. The average particle size, based on more than 100 particles in Fig. 4C, is 2.3 nm, which agrees well with the XRD results. The particle sizes are markedly smaller than what has been reported in the literature under similar conditions [26]. The as-prepared MW-PC TEM images resemble those of H-MW-PC (not shown here), indicating that the mild heat treatment after preparation had no adverse effects on the particle size distribution or particle sizes.

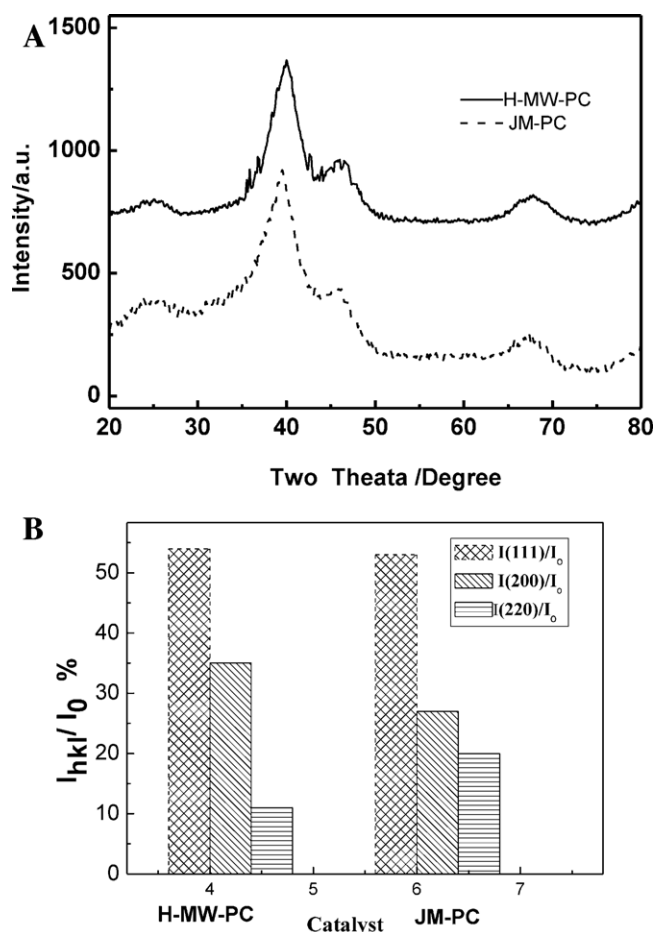


Fig. 3. XRD patterns of the H-MW-PC and JM-PC (A) and  $I_{hkl}/I_0$  ratio of the catalysts (B).

Fig. 5 displays the cyclic voltammograms (CVs) of H-MW-PC, JM-PC, and the as-prepared MW-PC catalyst without post-treatment in  $0.5\text{ mol L}^{-1}\text{ H}_2\text{SO}_4$  solution. All CVs in this work are normalized to the geometric surface area. The integrated charge in the hydrogen absorption region of the CVs is used to calculate the electrochemical surface areas (ESA), using the recognized formula and assuming a correlation value of  $0.21\text{ mC cm}^{-2}$  (calculated from a surface density of  $1.3 \times 10^{15}\text{ at cm}^{-2}$ , a value generally admitted for polycrystalline Pt electrodes):

$$\text{ESA} = \frac{Q_H}{0.21 \times 10^{-3} \times m}$$

where  $Q_H$  is the amount of charge exchanged during the adsorption of hydrogen atoms on the Pt surface (C) and  $m$  is the platinum loading in the electrode ( $\text{g cm}^{-2}$ ). Assuming spherical Pt nanoparticles, the chemical surface area (CSA) in  $\text{m}^2\text{ g}^{-1}$  and the Pt utilization efficiency for these catalysts can be calculated using the following formulae:

$$\text{CSA} = \frac{6000}{\rho \times d}$$

$$\text{Pt utilization efficiency (\%)} = \frac{\text{ESA}}{\text{CSA}} \times 100$$

where  $\rho$  is the platinum density ( $21.4\text{ g cm}^{-3}$ ) and  $d$  is the average particle size of the Pt nanoparticles (nm). The corresponding ESA, CSA, and Pt utilization efficiency for H-MW-PC, JM-PC, and the as-prepared MW-PC catalyst are listed in Table 1.

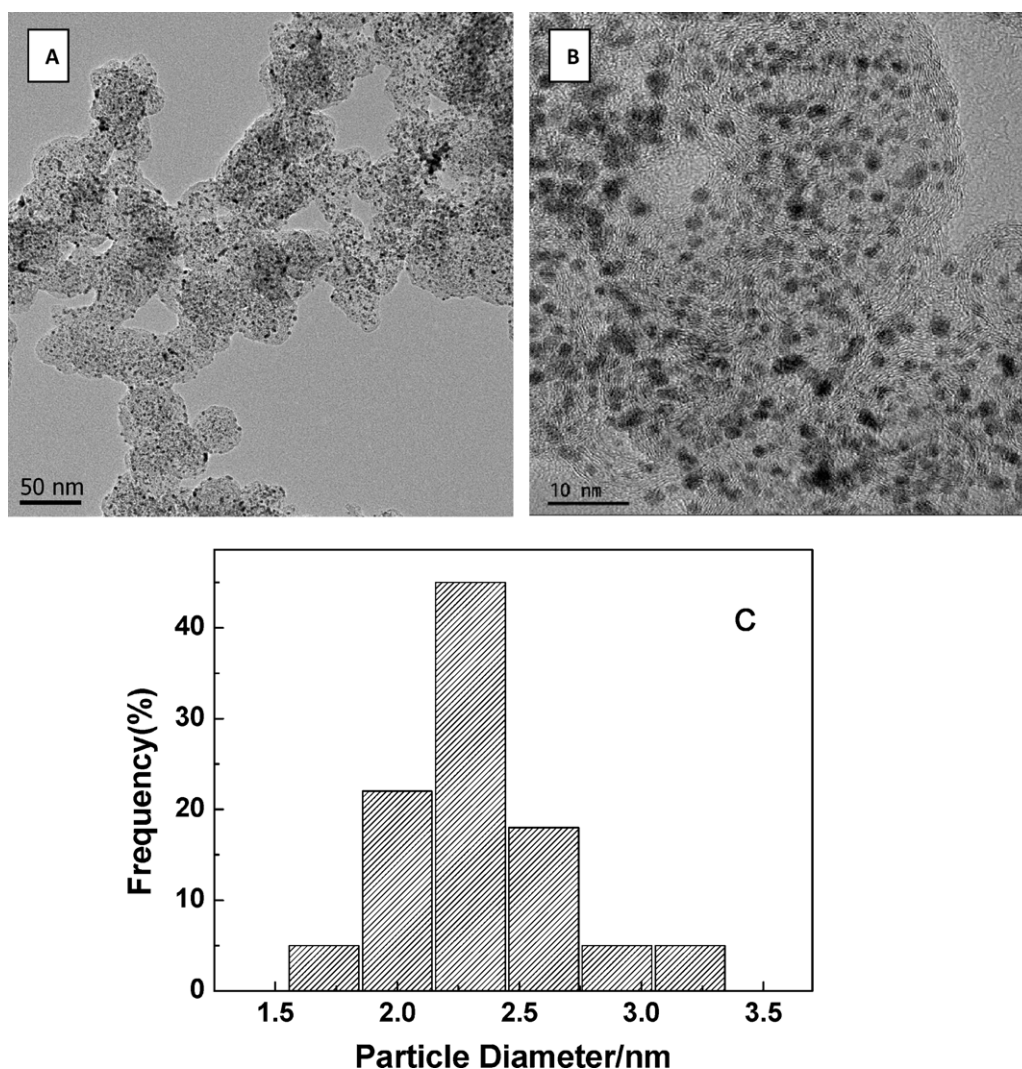


Fig. 4. TEM images of H-MW-PC with different magnifications (A and B) and the corresponding particle size distribution of H-MW-PC (C).

As is clearly evident in Table 1, although the Pt loading of H-MW-PC is high, up to 40%, the ESA and Pt utilization efficiency are  $104 \text{ m}^2 \text{ g}^{-1}$  and 85.9%, respectively – 10% higher than for the JM-PC catalyst. It should be noted that this activity enhancement is based on volume production up to 3 g per pot, which is quite meaningful in terms of practical application. Compared with the as-prepared catalyst, the post-treatment using heat and in a combination of different atmospheres ( $\text{N}_2$ ,  $\text{O}_2$ , and  $\text{H}_2$  in turn) increased the ESA and Pt utilization efficiency of H-MW-PC. We can speculate on the reasons for these enhancements. Some Pt atoms are likely to be covered by certain surface moieties during the course of catalyst preparation, making these Pt atoms unable to participate in the surface reaction. Heat treatment in a  $\text{N}_2$  atmosphere may remove these surface species and release more active surface sites. On the other hand, possible residual organic compounds incident in the preparation

process may be oxidized to purify the as-prepared catalyst, yielding increased activity. Lastly, hydrogen purging in the second stage reduces any active compounds on the Pt, converting it to a more reduced state. As a combined result, the H-MW-PC catalyst heat

**Table 1**  
Comparisons of particle size, ESA, CSA, and Pt utilization of the catalysts.

Catalyst	Pt particle size (nm)	ESA ( $\text{m}^2 \text{ g}^{-1}$ )	CSA ( $\text{m}^2 \text{ g}^{-1}$ )	Pt utilization efficiency (%)
H-MW-PC	2.3	104	122	85.9
JM-PC	2.4	91	117	77.6
MW-PC	2.3	83	122	68.0

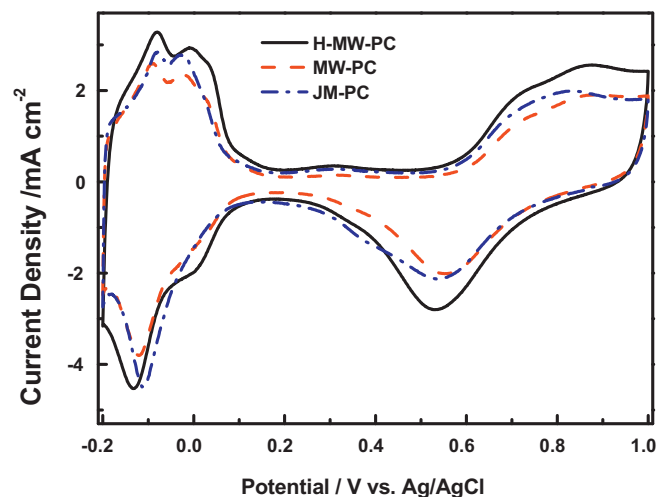


Fig. 5. Cyclic voltammograms of H-MW-PC, JM-PC, and the as-prepared MW-PC catalyst in  $0.5 \text{ mol L}^{-1} \text{ H}_2\text{SO}_4$  solution.

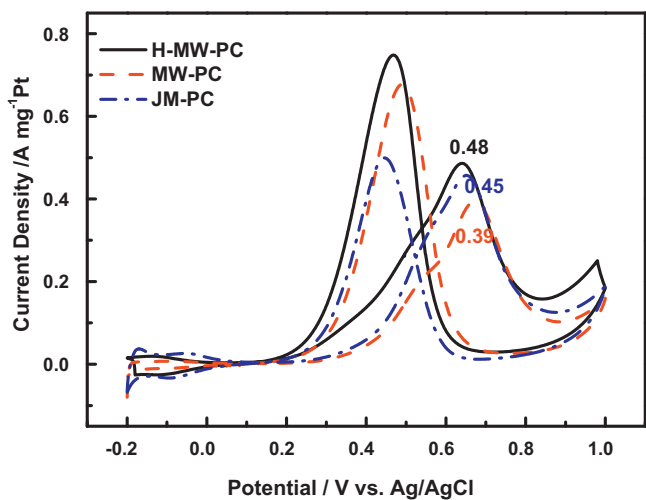


Fig. 6. Room-temperature cyclic voltammograms of the catalysts in  $0.5 \text{ mol L}^{-1} \text{ H}_2\text{SO}_4 + 0.5 \text{ mol L}^{-1} \text{ CH}_3\text{OH}$ .

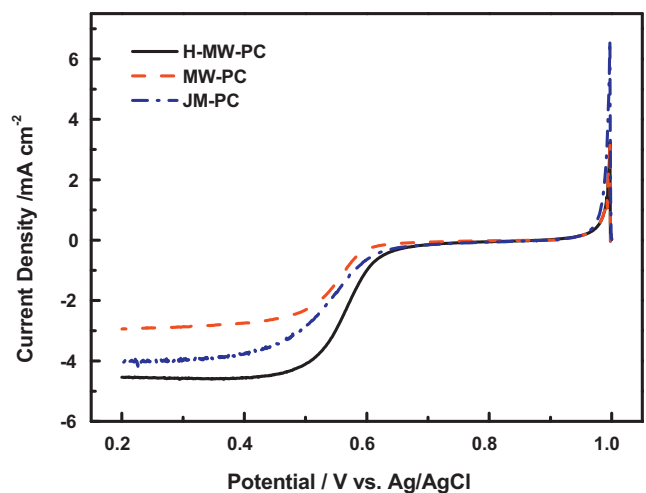


Fig. 7. Polarization curves of the oxygen reduction reaction in oxygen-saturated  $0.5 \text{ mol L}^{-1} \text{ H}_2\text{SO}_4$ .

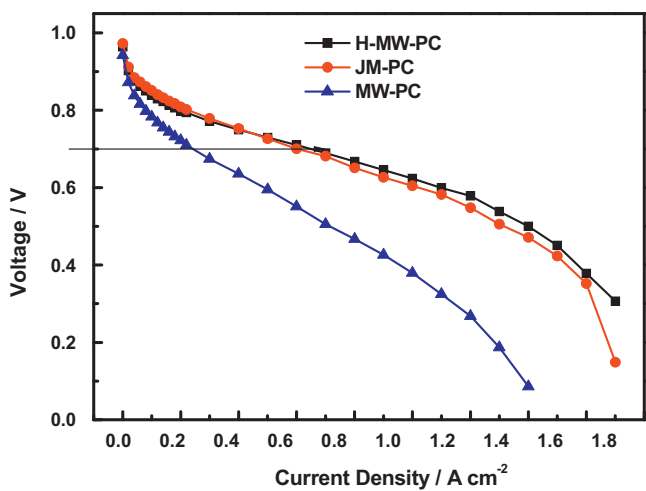


Fig. 8. Performances of MEAs prepared with different cathode catalysts in a  $\text{H}_2/\text{air}$  single fuel cell.

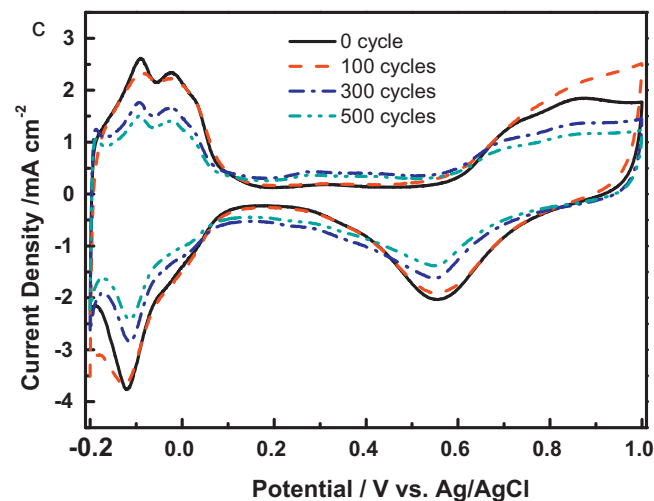
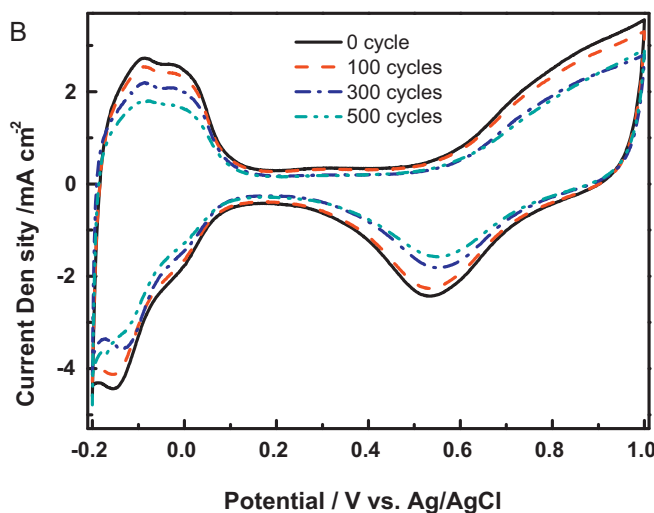
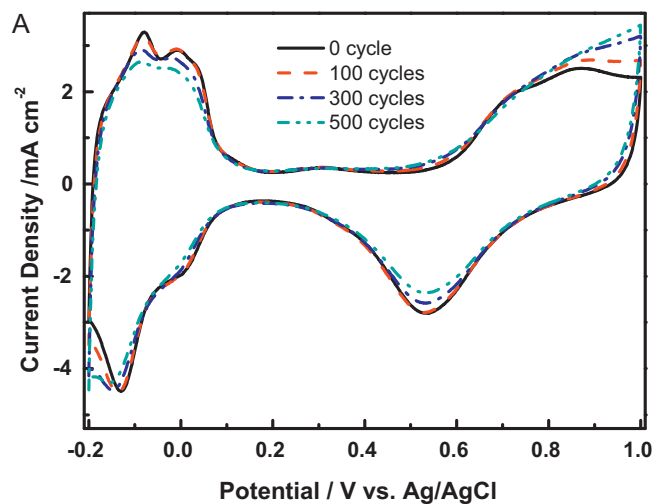


Fig. 9. Room-temperature cyclic voltammograms obtained in  $0.5 \text{ mol L}^{-1} \text{ H}_2\text{SO}_4$  after 500 cycles for the catalysts: (A) H-MW-PC, (B) JM-PC, and (C) MW-PC.

treated in different atmospheres showed higher activity than the as-prepared one.

Fig. 6 shows the CVs of methanol electrooxidation for the as-prepared catalyst, H-MW-PC, and JM-PC in a solution of  $0.5 \text{ mol L}^{-1} \text{ CH}_3\text{OH} + 0.5 \text{ mol L}^{-1} \text{ H}_2\text{SO}_4$ . It can be observed that the peak current density in the forward scan for H-MW-PC is  $0.48 \text{ A mg}^{-1} \text{ Pt}$ , higher than that of JM-PC ( $0.45 \text{ A mg}^{-1} \text{ Pt}$ ) and the as-prepared MW-PC catalyst ( $0.39 \text{ A mg}^{-1} \text{ Pt}$ ). Furthermore, the methanol oxidation onset potential on H-MW-PC is  $0.18 \text{ V}$ , negatively shifted  $40 \text{ mV}$  compared with that of JM-PC. The superior methanol oxidation catalytic activity and lower onset potential of H-MW-PC compared with JM-PC may result from the increase in Pt utilization efficiency brought about by its high ESA and high dispersion of Pt on the carbon support. It is perhaps worth noting that the particle sizes in the carbon support used for the JM-PC catalyst are about  $20 \text{ nm}$ , much smaller than in the Vulcan XC72 carbon support ( $50\text{--}100 \text{ nm}$ ) used in this work. Although Vulcan XC72 may provide fewer possible support areas, we can still use this kind of carbon to prepare a catalyst that displays enhanced activity (compared with the state-of-the-art Johnson Matthey catalysts).

The polarization curves for the oxygen reduction reaction of the catalysts in oxygen-saturated  $0.5 \text{ mol L}^{-1} \text{ H}_2\text{SO}_4$  are given in Fig. 7, and show that the oxygen reduction activity of H-MW-PC and JM-PC is comparable. Fig. 8 shows the performance of three MEAs using H-MW-PC, as-prepared MW-PC, and JM-PC as the respective cathode catalysts. It is clear that the cell performance with H-MW-PC was significantly better than with the as-prepared catalyst. In a hydrogen-air single fuel cell, the current density of the MEA with H-MW-PC was  $630 \text{ mA cm}^{-2}$  ( $0.7 \text{ V}$ ), which was higher than that of the MEA prepared with JM-PC under identical conditions. These results are in agreement with the expectation that H-MW-PC with more exposed Pt (2 0 0) lattice planes may have superior activity for oxygen reduction. It is well known that for electrocatalysts in practical applications, stability or durability is a very important factor in evaluating catalytic performance. To evaluate the catalysts' stability, we conducted an accelerated durability test. Specifically, the catalysts were scanned between  $-0.2 \text{ V}$  and  $1.0 \text{ V}$  for 500 cycles in  $0.5 \text{ mol L}^{-1} \text{ H}_2\text{SO}_4$  and the ESAs were recorded every 100 cycles. Fig. 9 shows the CVs thus obtained. It can be seen that after 500 cycles, the ESA losses for H-MW-PC, JM-PC, and MW-PC were 17.6%, 31.8%, and 45.3%, respectively, indicating the superior stability of H-MW-PC.

#### 4. Conclusion

A high-loading (40 wt.%), high-performance Pt/C catalyst has been prepared by a microwave-assisted organic colloid approach.

Despite this high metal loading, Pt nanoparticles were dispersed on a Vulcan XC72 carbon support with a uniform size distribution and an average particle size of  $2.3 \text{ nm}$ . The catalyst's performance was found to surpass that of Johnson Matthey Pt/C for both methanol oxidation and oxygen reduction. In a hydrogen-air single fuel cell, the current density of the MEA with the homemade catalyst reached  $630 \text{ mA cm}^{-2}$  ( $0.7 \text{ V}$ ), which is comparable with state-of-the-art Johnson Matthey Pt/C.

#### Acknowledgements

The authors gratefully acknowledge the financial support provided by the National Natural Science Foundation of China (Project nos. 20876062 and 21076089).

#### References

- [1] C. Bock, C. Paquet, M. Couillard, G.A. Botton, B.R. MacDougall, *J. Am. Chem. Soc.* 126 (2004) 8028–8037.
- [2] S. Liao, K.-A. Holmes, H. Tsapralis, V.I. Birss, *J. Am. Chem. Soc.* 128 (2006) 3504–3505.
- [3] X. Yu, S. Ye, *J. Power Sources* 172 (2007) 133–144.
- [4] T.S. Ahmadi, Z.L. Wang, T.C. Green, A. Henglein, M.A. El-Sayed, *Science* 272 (1996) 1924–1925.
- [5] H.B. Bonnemant, N.W. Waldofner, H.G. Haubold, T. Vad, *Chem. Mater.* 14 (2002) 1115–1120.
- [6] Z.Q. Tian, F.Y. Xie, P.K. Shen, *J. Mater. Sci.* 39 (2004) 1507–1509.
- [7] C. Liu, X. Xue, T. Lu, W. Xing, *J. Power Sources* 161 (2006) 68–73.
- [8] R. Ramkumar, S. Dheenadayalan, R. Pattabiraman, *J. Power Sources* 69 (1997) 75–80.
- [9] R.Z. Jiang, C. Rong, D.R. Chu, *Electrochim. Acta* 56 (2010) 2532–2540.
- [10] C. Rong, R.Z. Jiang, W. Sarney, D. Chu, *Electrochim. Acta* 55 (2010) 6872–6878.
- [11] H. Liu, C. Song, L. Zhang, J. Zhang, H. Wang, D.P. Wilkinson, *J. Power Sources* 155 (2006) 95–110.
- [12] H. Cheng, W. Yuan, K. Scott, *Fuel Cells* 7 (2007) 16–20.
- [13] F. Coloma, A. Sepulveda-Escribano, J.L.G. Fierro, F. Rodriguez-Reinoso, *Langmuir* 10 (1994) 750–755.
- [14] M. Kang, Y.-S. Bae, C.-H. Lee, *Carbon* 43 (2005) 1512–1516.
- [15] M. Mazurek, N. Benker, C. Roth, H. Fuess, *Fuel Cells* 6 (2006) 208–213.
- [16] J.H. Tian, F.B. Wang, Z.Q. Shan, R.J. Wang, J.Y. Zhang, *J. Appl. Electrochem.* 34 (2004) 461–467.
- [17] E. Antolini, F. Cardellini, E. Giacometti, G. Squadrito, *J. Mater. Sci.* 37 (2002) 133–139.
- [18] E. Antolini, *J. Mater. Sci.* 38 (2003) 2995–3005.
- [19] K.S. Han, Y.-S. Moon, O.H. Han, K.J. Hwang, I. Kim, H. Kim, *Electrochem. Commun.* 9 (2007) 317–324.
- [20] J.M. Liu, H. Meng, J.L. Li, S.J. Liao, J.H. Bu, *Fuel Cells* 7 (2007) 402–407.
- [21] T. Teranishi, M. Hosoe, T. Tanaka, M. Miyake, *J. Phys. Chem. B* 103 (1999) 3818–3827.
- [22] S.-Y. Zhao, S.-H. Chen, S.-Y. Wang, D.-G. Li, H.-Y. Ma, *Langmuir* 18 (2002) 3315–3318.
- [23] J. Zeng, J.Y. Lee, J. Chen, P.K. Shen, S. Song, *Fuel Cells* 7 (2007) 285–290.
- [24] N. Markovic, H. Gasteiger, P.N. Ross, *J. Electrochem. Soc.* 144 (1997) 1591–1597.
- [25] C.Z. He, H.R. Kunz, J.M. Fenton, *J. Electrochem. Soc.* 144 (1997) 970–979.
- [26] S. Song, Y. Wang, P.K. Shen, *J. Power Sources* 170 (2007) 46–49.